Power Line Transient Interferences on a Nearby Pipeline Due to a Lightning Discharge

Amauri G. Martins-Britto, Sébastien R. M. J. Rondineau, Felipe V. Lopes

Abstract—This paper discusses basic concepts of the lightning phenomena and lightning protection systems (LPS) commonly employed in power lines, and its resulting impacts on a neighboring structure, such as a pipeline. A finite-difference time-domain (FDTD) implementation is employed to simulate the transient interferences produced by the power line due to a lightning strike, with emphasis on safety aspects and risks to which the pipeline is exposed. The distribution of the discharge currents along the grounding conductors is investigated, as well as the resulting ground potential rise, caused by the injection of electrical current into the earth. Results show that a significant portion of the ground potential is transfered to the pipeline in the form of stress voltages, exceeding nominal limits of the insulating coating and equipment connected to the pipeline. Also, the dangers to which people are exposed in the vicinities of the tower, in the form of touch and step voltages, are highlighted, along with possible strategies to mitigate these hazards.

Keywords—Finite-difference time-domain (FDTD) method, grounding grid, lightning discharge, power line, pipeline, electromagnetic interference.

I. INTRODUCTION

OVERHEAD transmission lines are a critical component of any power transmission or distribution system. They are large installations, often subject to extreme conditions, that affect and are affected by its surroundings. Underground pipelines have the same characteristics and, due to progressively stricter environmental regulations, there is a world-wide trend of sharing common spaces among power lines and utility lines, creating the so-called right-of-ways [1].

Lightning discharges are a well-known cause of failure of both systems [2], [3]. A direct discharge on a power line or induced voltages caused by a lightning strike on its vicinities may provoke line flashover or insulation failure of transformers, arresters or other equipment, ultimately leading to power outage, what justifies the adoption of measures such as installation of shield wires. On pipelines, lightning strikes may cause damage to the pipe, appurtenances, insulating joints and coatings, as well as potentially hazardous voltages for living beings.

An underground pipeline exposed to the energized conductors of a power line is subject to a variety of phenomena, which results in induced voltages throughout its course, due to inductive and conductive coupling mechanisms, both in steady-state and transient conditions [4], [5]. This

paper focuses on a hypothetical case where a lightning discharge strikes the shield wires of a power line and is conducted to the earth through the tower structure and grounding conductors, giving cause to a ground potential rise (GPR) and its effects on an adjacent pipeline.

A review of basic lightning discharge and protection mechanisms is provided, after which the finite-difference time-domain (FDTD) method is employed to investigate the transient voltages induced on the pipeline by the lightning discharge currents flowing through the power line conductors. The FDTD code has been fully developed by the authors in order to specifically handle lightning current waveforms, and validated in a previous study by means of comparison with results reported in the literature [6].

Of practical interest to the industries of energy, oil & gas, ore and water distribution/sanitation, this work is expected to contribute with techniques to predict and mitigate risks to which people and pipelines are exposed, thus assisting in the design of safer facilities, with technically feasible and economical solutions.

II. BASICS OF LIGHTNING DISCHARGES AND PROTECTION

Lightning is a sudden electrostatic discharge that occurs typically during a thunderstorm. An electrically active thundercloud may be regarded as an electrostatic generator suspended in an atmosphere of low electrical conductivity [7].

As a thundercloud moves over the surface of the Earth, an equal electric charge, but of opposite polarity, is induced on the Earth's surface underneath the cloud. The oppositely charged regions create an electric field within the air between them – the greater the accumulated charge, the higher the electric field. If the electric field intensity reaches the air breakdown field strength, whose magnitude is of the order of 3 MV/m, the discharge occurs. Lightning discharges may reach up to 30 million volts at 100 thousand amperes, during a time period of the order of microseconds [7].

Lightning protection systems (LPS) are used to prevent or mitigate lightning strike damage to structures by intercepting such strikes and safely conducting discharge currents to the ground. A lightning protection system often includes a network of air terminals, bonding conductors and ground electrodes designed to provide a low impedance path to the ground, from which follows that the grounding grid is the critical component of an LPS.

Overhead power lines are commonly equipped with a shield or earth wire, as depicted in Fig. 1, which is a bare conductor grounded at the top of each tower structure, in order to

reduce the probability of direct lightning strikes on the phase conductors.
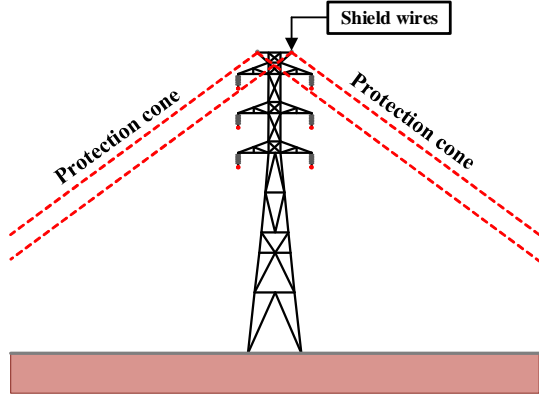

Fig. 1. Shield wires on the top of a power line, parallel to the phase conductors, made of bare wires with a direct connection to the tower structure, designed to intercept lightning discharges and conduct surge currents to the ground. Shield wires provide a protection cone, under which structures, such as the phase conductors, are shielded against lightning strokes.

III. MATHEMATICAL MODEL

A. Review of the FDTD method

Since the focus of this paper is the FDTD application in a practical situation, only a brief description of the method is provided. For the interested reader, reference [8] contains an in-depth step-by-step explanation of a complete FDTD implementation.

The FDTD method provides a direct approximation of Maxwell equations by means of central finite differences, which are evaluated for electrically small discrete subdomains [9]. Referring to the geometry shown in Fig. 2, the time-domain solution to Maxwell equations is obtained using the modified Yee algorithm, expressed in (1)-(8) [8], [9].
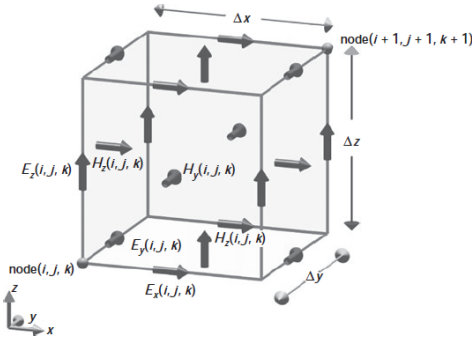

Fig. 2. Representation of Yee lattice with modified node numbering, reproduced from [8]. The FDTD technique divides the three-dimensional problem geometry into cells to form a grid, allowing for the representation of Maxwell time-dependent curl equations in discrete form, both in space and time, employing the second-order accurate central difference formula.

$$H_x^n(i,j,k) = H_x^{n-1}(i,j,k) + \tilde{E}_y^{n-1}(i,j,k+1) - \tilde{E}_y^{n-1}(i,j,k) - \tilde{E}_z^{n-1}(i,j+1,k) + \tilde{E}_z^{n-1}(i,j,k), \tag{1}$$

$$H_y^n(i,j,k) = H_y^{n-1}(i,j,k) + \tilde{E}_z^{n-1}(i+1,j,k) - \tilde{E}_z^{n-1}(i,j,k) - \tilde{E}_x^{n-1}(i,j,k+1) + \tilde{E}_x^{n-1}(i,j,k), \tag{2}$$

$$H_y^n(i,j,k) = H_z^{n-1}(i,j,k) + \tilde{E}_x^{n-1}(i,j+1,k) - \tilde{E}_x^{n-1}(i,j,k) - \tilde{E}_y^{n-1}(i+1,j,k) + \tilde{E}_y^{n-1}(i,j,k), \tag{3}$$

$$\tilde{E}_x^n(i,j,k) = C_a(m)\tilde{E}_x^{n-1}(i,j,k) + C_b(m)[H_z^{n-1}(i,j,k) - H_z^{n-1}(i,j-1,k) - H_y^{n-1}(i,j,k) + H_y^{n-1}(i,j,k-1)], \tag{4}$$

$$\tilde{E}_x^n(i,j,k) = C_a(m)\tilde{E}_y^{n-1}(i,j,k) + C_b(m)[H_x^{n-1}(i,j,k) - H_x^{n-1}(i,j,k-1) - H_z^{n-1}(i,j,k) + H_z^{n-1}(i-1,j,k)], \tag{5}$$

$$\tilde{E}_z^n(i,j,k) = C_a(m)\tilde{E}_z^{n-1}(i,j,k) + C_b(m)[H_y^{n-1}(i,j,k) - H_y^{n-1}(i-1,j,k) - H_x^{n-1}(i,j,k) + H_x^{n-1}(i,j-1,k)], \tag{6}$$

$$R = \frac{\Delta t}{2\varepsilon_0}, R_a = \left(\frac{c\Delta t}{\Delta}\right)^2, R_b = \frac{\Delta t}{\mu_0\Delta}, \tilde{E} = R_b\vec{E} \tag{7}$$

$$C_a = \frac{1 - R\sigma(i,j,k)/\epsilon_r(i,j,k)}{1 + R\sigma(i,j,k)/\epsilon_r(i,j,k)}, C_b = \frac{R_a}{\epsilon_r(i,j,k)R\sigma(i,j,k)}, \tag{8}$$

where subscripts x, y and z denote the respective components of the magnetic field $\vec{H}$, in A/m, and electric field $\vec{E}$, in V/m; ε is the electric permittivity, in F/m; μ is the magnetic permeability, in H/m; Δt is the time-step, in s; c is the speed of light, in m/s; Δ is the space discretization unit, in m; and σ is the electric conductivity, in S.

The time-increment Δt in equations above must satisfy the following stability condition, also known as Courant condition:

$$c_{max}\Delta t = \left[\frac{1}{\Delta x^2} + \frac{1}{\Delta y^2} + \frac{1}{\Delta z^2}\right]^{-\frac{1}{2}}, \tag{9}$$

where c_{max} is the maximum wave propagation velocity within the domain and Δx, Δy and Δz are the domain space discretization units [8].

With the modified algorithm, the electromagnetic fields are determined by setting all components in the domain equal to 0 for $t \leqslant 0$ and iterating equations above over the desired time period.

Modeling an open FDTD problem requires special techniques in order to accurately represent the system under study, namely absorbing boundary conditions (ABCs). There is a wide range of methods available for this purpose, however, the perfectly matched layer (PML) introduced by Berenger has been proven to be one of the most robust ABCs in comparison with other techniques adopted in the past [8], [10]. The PML technique consists of surrounding the computational domain with a finite-thickness material based on fictitious constitutive parameters to create a wave-impedance matching condition, which is independent of the angles and frequencies of the wave incident on each boundary.

The FDTD method is recognized as a powerful tool, although computationally expensive, to solve a variety of electromagnetism problems, with reports of successful applications to lightning discharge and electrical grounding studies [6], [11]. One key aspect of the FDTD that is worth to mention is the ability to intrinsically handle heterogeneities,

such as layered structures and finite volumes of solids with different constitutive parameters, which allows for the construction of complex, realistic simulation models.

B. Lightning discharge model

The lightning current pulse is characterized by a peak value, rise time and half-value time and is approximated by the Heidler function (10), which accounts for the concave behavior of the rising portion of a typical lightning stroke [12]:

$$I_s(t) = \frac{I_0}{\eta} \frac{(t/\tau_1)^n}{1 + (t/\tau_1)^n} e^{(-t/\tau_2)}, \qquad (10)$$

where I_0 is the current amplitude at the base of the lightning channel, in A; τ_1 is the rise time constant, in s; τ_2 is the half-value time constant, in s; n is an integer $(1, 2,...,10)$; and η is the current amplitude correction factor, given by:

$$\eta = e^{[(\tau 1/\tau 2)(n\tau 1/\tau 2)]^{-1/n}}. \qquad (11)$$

For the simulations in this paper, it is adopted a pulse with peak value 30 kA, $\tau_1 = 1$ μs, $\tau_2 = 50$ μs and $n = 1$, values reported as typical of lightning strokes with moderate amplitude [13]. The respective current waveform is shown in Fig. 3.

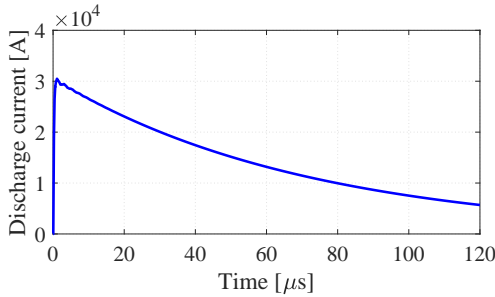Fig. 3. Lightning discharge waveform, with peak magnitude 30 kA, rise time 1 μs and half-value time 50 μs.

In order to introduce $I_s(t)$ into the FDTD model, a current source and a loop electrode with ground return path are employed [11]. The loop electrode is positioned at a remote location from the system under study (e.g. distance > 100 m) to simulate the discharge current in a practical situation, as illustrated in Fig. 4.
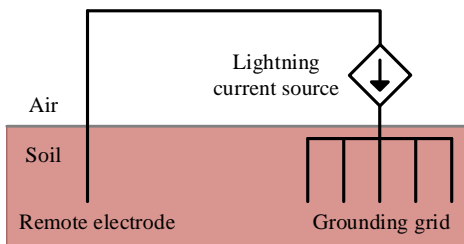

Fig. 4. Lightning equivalent current source. Source injects into the grounding grid the current with waveform shown in Fig. 3. The circuit is completed through an electrode placed sufficiently far from the grounding grid, with ground return path. For this work, a distance of 100 m is adopted.

IV. SIMULATIONS

A. System description

The power line under study, whose perspective view is given in Fig. 5, is composed of the tower structure, phase conductors, shield wires, grounding conductors (counterpoises), and the concrete foundations and respective steel-frames.
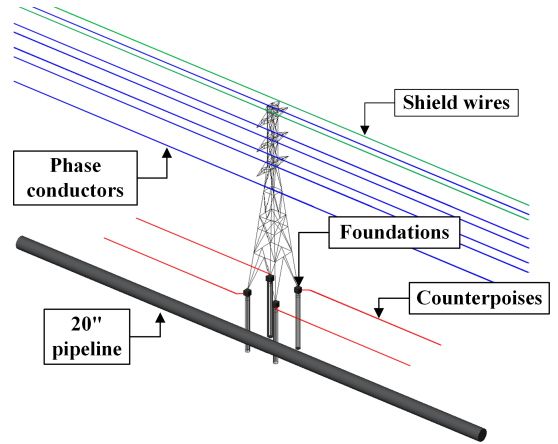

Fig. 5. Perspective view of the system under study. The pipeline is parallel to the transmission line, with a separation distance of 10 m. A lightning discharge is assumed to hit the top of tower, being conducted to the ground through the tower structure, counterpoises and tower foundations.

The transmission line shares the right-of-way with a 20" diameter underground carbon steel pipeline, coated with 3-layer polyethilene (3LPE), installed at 3.5 m depth, which runs parallel to the transmission line axis, with a horizontal separation of 10 m. Figs. 6 and 7 provide schematic views with the most relevant dimensions.
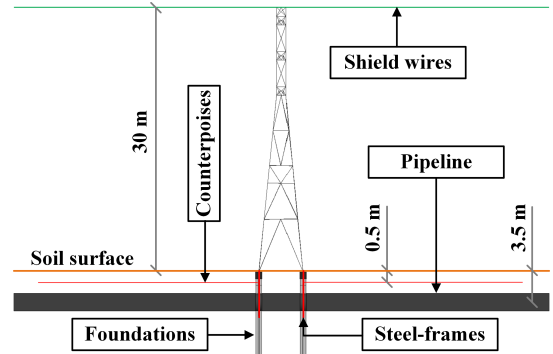

Fig. 6. Side view showing the pipeline, counterpoises, burial depths, tower structure, concrete foundations and steel-frames. Tower height is 30 m from the soil surface. Pipeline and counterpoises are buried, respectively, at 3.5 m and 0.5 m. Foundations are 10 m long with steel-frames of 3 m.
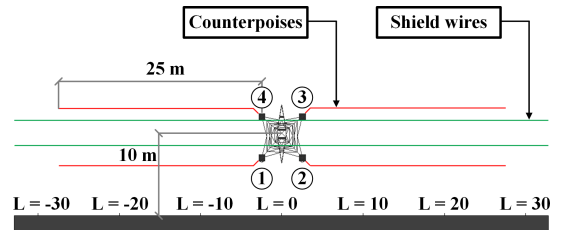

Fig. 7. Top view showing counterpoises lengths, horizontal spacing, foundations and observation points. Currents injected into the ground are sampled at points 1 to 4. Ground potential rise is sampled at points L=-30 to L=30.

Tables I and II summarize the constitutive properties and dimensions of the materials used. For conductors, the thin-wire approximation is used [8]. The concrete foundations are

modeled as solid cylinders with diameter 70 cm, length 10 m below the soil surface, which is assumed to be at $z = 0$. The counterpoises are 25 m long, buried at 50 cm depth. The tower height is 30 m. The lightning discharge is assumed to strike the top of the tower.

Description	Material	σ (S/m)	ε_r	μ_r
Phase conductors	ACSR Grosbeak	2.5417×10^7	1	1.064
Shield wires	EHS Steel	4.0904×10^6	1	63.29
Tower structure	EHS Steel	4.0904×10^6	1	63.29
Counterpoises	Annealed copper	5.8001×10^7	1	1
Soil layer	Dry clay	2×10^{-3}	10	1
Foundations	Dry concrete	1×10^{-6}	4.5	1
Steel-frame	EHS Steel	4.0904×10^6	1	63.29
Pipeline wall	Carbon Steel	5.8001×10^6	1	300
Pipeline coating	Polyethilene	1×10^{-12}	2.25	1

TABLE II

DIMENSIONS OF CONDUCTORS

Description	Radius (m)
Phase conductors	1.2570×10^{-2}
Shield wires	0.4572×10^{-2}
Tower structure	0.05
Counterpoises	0.4572×10^{-2}
Pipeline	0.25

B. FDTD domain

The FDTD domain is a rectangular parallelepiped with dimensions $145 \times 105 \times 82.5$ m, with a discretization resolution of 50 cm. An air buffer of 5 m is added to each domain dimension, under 10 extra cells of PML materials. The domain is centered on the tower of interest. Fig. 8 shows a discrete domain representation of Fig. 5. Simulation is carried out over 120 μs, with a timestep of 866 ps in order to comply with the stability criterion described in (9). A total computation time of approximately 121 h was required to run on an Intel® Core i9-7900X CPU @ 3.3 GHz with 64 GB RAM, which justifies the decision made by the authors of modeling the effects of a single tower, since increasing the domain size to include more structures would make necessary a considerably higher computing time.

C. Results

Sampled values are the currents injected into the soil by the grounding conductors and tower foundations, numbered from 1 to 4 in Fig. 7, transient ground potential rise and coating stress voltages at 7 observation points, labeled as $L = -30$ to $L = 30$ in Fig. 7, as well as touch and step voltages near the tower vicinities. Ground potentials are computed as the line integral of the electric field at the soil surface, from the observation point to the extremity of the domain, following the y-axis. Coating stress voltages are calculated as the line integral of the electric field along the z-direction, from the pipe wall cell to the soil cell immediately above the pipe.
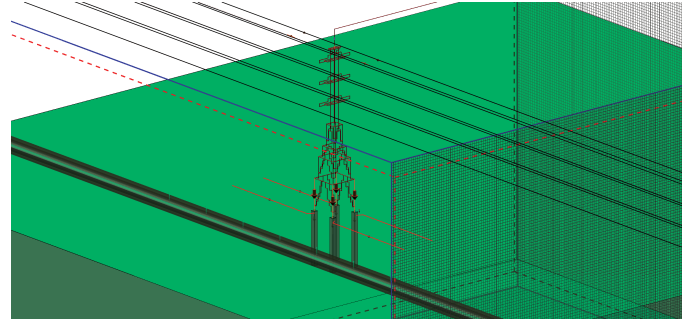

Fig. 8. Model built for the FDTD simulations showing the pipeline, counterpoises, tower and foundations of Fig. 5 in the discretized domain. Cell size is $\Delta x = \Delta y = \Delta z = 50$ cm. The pipeline is modeled as 3 concentric cylinders, corresponding, respectively, to the inner region of the pipe (air), the metallic wall and the pipeline coating. Foundations are modeled as solid cylinders made of concrete.

Figs. 9 and 10 present, respectively, the currents injected into the soil by the counterpoises and the tower foundations.
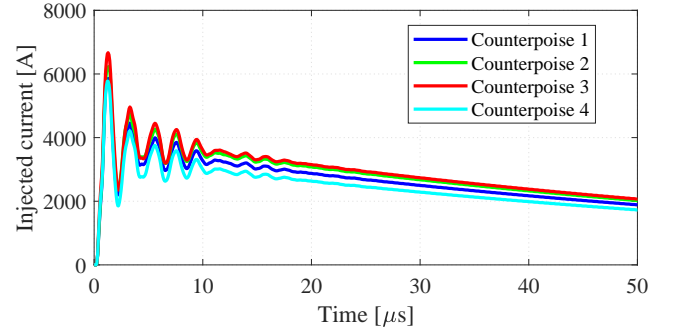

Fig. 9. Currents injected into the soil by the counterpoises. Curves follow the trend of the lightning discharge (Fig. 3), with a maximum value of 6.6 kA being injected by counterpoise 3. Transients are more intense over the first 10 μs.
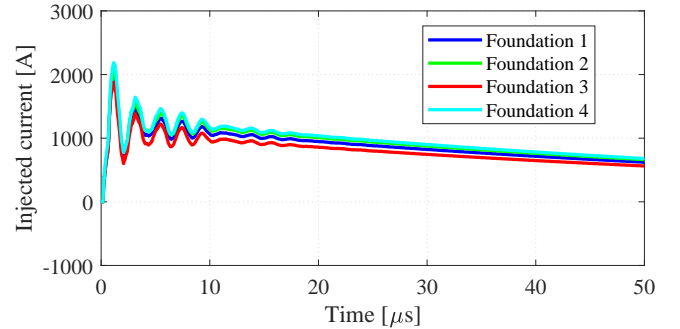

Fig. 10. Currents injected into the soil by the tower foundations. Values are of the order of 32% of the ammount discharged by the counterpoises, even though the dry concrete is a poor conductor. Foundation 3 injects the maximum current of 2.1 kA.

Figs. 9 and 10 indicate that the counterpoises play the most significant role in discharging the lightning current to the ground, as expected, since it is the controlled grounding structure. However, the contribution of the tower foundations, of the order of 32% of the current flowing through the counterpoises, is not to be neglected, even though the concrete

in dry conditions is a poor conductor.

As a consequence of the current injection into the earth, a ground potential rise occurs, which is transfered to the pipeline as a result of the conductive coupling between the grounding conductors and the pipe metal. Figs. 11 and 12 show, respectively, the ground potential rise and the pipeline coating stress voltages at the observation points. Figures are zoomed into the first 10 μs, which Figs. 9 and 10 demonstrate to be the period within which the transients reach the most significant magnitudes.

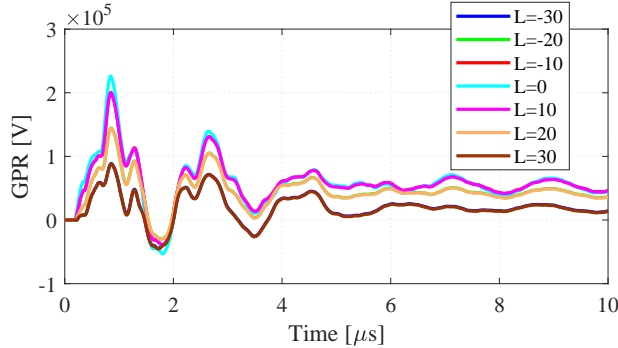Fig. 11. Ground potential rise at observation points over the first 10 μs. Maximum value is of the order of 226 kV at point $L = 0$, $t = 1$ μs, which agrees with the fact that this observation point is the closest to the current source. Values are consistent with the simplified analytical expression (12).
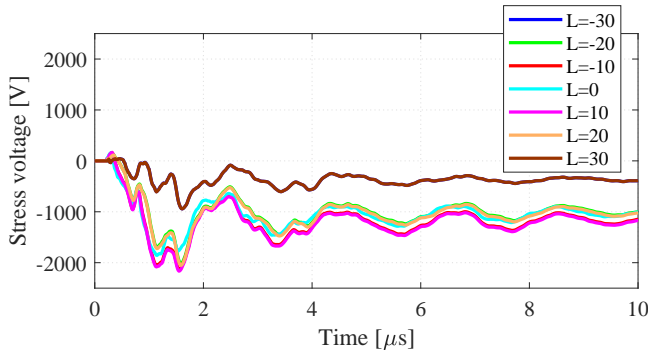

Fig. 12. Pipeline coating stress voltages at observation points for the first 10 μs. Maximum absolute value is 2.1 kV, which exceeds the tolerable limit of the pipeline coating (2 kV) and equipment connected to the pipeline, such as rectifiers (1.5 kV) and insulating flanges (1 kV).

Fig. 11 shows that the GPR reaches a maximum value of 226 kV at observation point $L = 0$. In order to verify the coherence of this result, a simple verification can be made: a grounding electrode in uniform soil, sufficiently far from the observation point, behaves as a point source and produces a GPR calculated as in (12) [4].

$$GPR = \frac{\rho I}{2\pi r},\qquad(12)$$

where $\rho = 500$ Ω.m is the soil resistivity for this case, $I = 30$ kA is the peak discharge current at $t = 1$ μs, and $r = 10$ m is the distance between the tower and the observation point $L = 0$, resulting in a GPR of 238 kV, which agrees with results above.

Fig. 12 indicates that the maximum stress voltage is of the order of 2.1 kV, which is potentially damaging to the

pipeline, depending on the type of coating (e.g. plastic tapes have a nominal limit of 2 kV), as well as to equipment commonly associated to it, for instance: cathodic protection rectifiers are designed to withstand a maximum voltage of 1.5 kV between the negative terminal and the metallic enclosure, whereas insulating flanges endure a maximum voltage of 1 kV [3], [5].

As the stress voltage is defined as the difference of potential between the pipe metal and the adjacent ground, it happens to be numerically equal to the touch voltage a person would be subject to, in case of a worker in contact with an equipment connected to the pipeline within the interference zone. Therefore, it is convenient to analyze the safe voltage limits, as given under IEEE Std. 80 [14]. Tables III and IV summarize results for different exposure times and scenarios:

TABLE III
TOLERABLE VOLTAGE LIMITS, BARE SOIL

Description	@ 20 μs (kV)	@ 60 μs (kV)	@ 100 μs (kV)
Touch voltage	45.39	26.20	20.3
Step voltage	103.75	59.90	46.4

TABLE IV
TOLERABLE VOLTAGE LIMITS, SOIL COVERED WITH INSULATING MATERIAL

Description	@ 20 μs (kV)	@ 60 μs (kV)	@ 100 μs (kV)
Touch voltage	541.27	312.50	242.06
Step voltage	2087	1.205	933.45

Tables above indicate that, although the potentials transfered to the pipeline are potentially damaging to the coating and equipment connected to the pipe, they range within the safe limits for humans, as long as very short exposure times are considered.

However, this is not the case for the touch voltage between the tower and the ground, shown in Fig. 13, as well as the step voltages near the grounding conductors, whose distribution is presented in Fig. 14. It is important to notice that Fig. 14 shows the electric field intensities at the soil surface, which are defined as the gradient of the scalar potentials, and, therefore, numerically equal to the step voltages.

Fig. 13 shows that the tower touch voltage reaches a maximum value of 171.4 kV, which is far above the tolerable limit according to Table III. The same happens with the step voltage, of the order of 94 kV. One possible strategy to mitigate these hazards is to cover the soil surface with an insulating material, e.g. a layer 10 cm thick of crushed rock. If the material resistivity is 20000 Ω.m, tolerable values increase, as can be verified from Table IV.

It is of relevance to observe that actual lightning surges may reach amplitudes as high as 200 kA [17]. Therefore, considerably higher induced voltages may be expected in practical situations.

V. CONCLUSIONS

This paper provided an overview of basic lightning discharge and protection mechanisms and a FDTD simulation of the transient interferences of an overhead power line on a
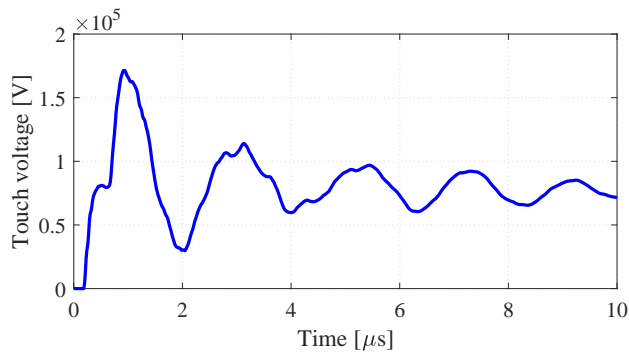
Fig. 13. Touch voltage at the tower vicinity. Maximum value of 171.4 kV exceeds the tolerable limits given in Table III. Covering the soil with a layer of crushed rock 10 cm thick increases the safe limit to 242 kV, according to Table IV, thus mitigating risks of eletrocution.
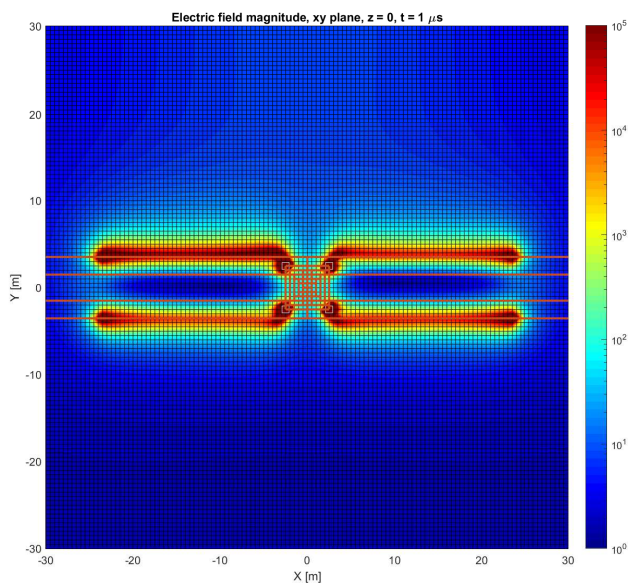

Fig. 14. Top view of the electric field magnitude at the soil surface, logarithmic color scale. The electric field is numerically equal to the step voltage, of which the maximum value of 94 kV exceeds the maximum step voltage limit. Highest magnitudes occur at the extremities of the conductors, which agrees with previous works where a similar grounding grid was simulated using the Method of Moments [5].

nearby pipeline due to a lightning stroke over the top of a tower.

A realistic model of the power line, accounting for phase conductors, shield wires, tower structure, counterpoises, concrete foundations and steel-frames, as well as the pipeline characteristics, was constructed. The lightning discharge was modeled as a current source with ground return path, in terms of a double exponential function with peak magnitude 30 kA, rise time 1 μs and half-value time 50 μs.

It was shown how the lightning discharge is dissipated into the earth through the shield wires, ground conductors and tower foundations, as well as the resulting impacts on the transmission line surroundings. Simulations indicated that the injection of current into the earth produces a ground potential rise, a significant portion of which is transfered to the pipeline by means of conductive coupling between the

grounding conductors and the pipe metal. Consequently, stress voltages arise throughout the pipeline course, with damaging potential to the pipeline and equipment connected to it. Also, potentially hazardous touch and step voltages appear at the tower vicinities.

This work provided a clear perspective of how resourceful the tools and techniques based on the electromagnetic theory can be when applied to power system transients, especially those related to lightning phenomena and electrical grounding. Further research and development will include the interferences resulting of the power line transient response in cases of a short-circuits to the ground.

REFERENCES

[1] G. C. Christoforidis, D. P. Labridis, and P. S. Dokopoulos, "Inductive interference calculation on imperfect coated pipelines due to nearby faulted parallel transmission lines," *Electric Power Systems Research*, vol. 66, no. 2, pp. 139–148, 2003.

[2] S. Das, S. Santoso, A. Gaikwad, and M. Patel, "Impedance-based Fault Location in Transmission Networks: Theory and Application," *IEEE Access*, vol. 2, pp. 537–557, 2014.

[3] NACE, "SP0177-2007 - Mitigation of Alternating Current and Lightning Effects on Metallic Structures and Corrosion Control Systems," pp. 1–25, 2007.

[4] WG-36.02, "Publication n. 95 - Guide on the Influence of High Voltage AC Power Systems on Metallic Pipelines," Paris, pp. 1–135, 1995.

[5] A. G. Martins-Britto, "Modeling of the Electromagnetic Interferences between Power Lines and Underground Metallic Pipelines and Impact Analysis," Master's Thesis, University of Brasília, 2017.

[6] A. G. Martins-Britto, S. R. M. J. Rondineau, and F. V. Lopes, "Transient Response of the Grounding Grid of a Power Line Tower Subject to a Lightning Discharge," in *WCNPS 2018: 3rd Workshop on Communication Networks and Power Systems*. Brasília, Brazil: IEEE Xplore, 2018.

[7] U. M. Rakov V.A., *Lightning: Physics and Effects*. Cambridge University Press, 2003.

[8] A. Elsherbeni and V. Demir, *The Finite-Difference Time-Domain Method for Electromagnetics with MATLAB® Simulations*, 2nd ed. SciTech Publishing, 2015.

[9] K. S. Yee, "Numerical Solution of Initial Boundary Value Problems Involving Maxwell's Equations in Isotropic Media," *IEEE Transactions on Antennas and Propagation*, vol. 14, no. 3, pp. 302–307, 1966.

[10] J.-P. Berenger, "Perfectly Matched Layer for the FDTD Solution of Wave-Structure Interaction Problem," *IEEE Transactions on Antennas and Propagation*, vol. 44, no. 1, pp. 110–117, 1996.

[11] J. Chen, F. Zhao, S. Zhou, and H. Tian, "FDTD Simulation of Lightning Current along Vertical Grounding Rod Appended to a Horizontal Grounding grid," 2010, pp. 1478–1481.

[12] IEC, "IEC 61312-1: Protection against lightning electromagnetic impulse - Part 1: General principles," 1995.

[13] D. W. Zipse, "Lightning Protection Systems: Advantages and Disadvantages," in *Industry Applications Society 40th Annual Petroleum and Chemical Industry Conference*, 1993. [Online]. Available: http://dx.doi.org/10.1016/B978-0-08-096921-3.15004-4

[14] IEEE Std 80, "Guide for Safety In AC Substation Grounding," pp. 1–192, 2000.

[15] "Standard Specification for ACSR Twisted Pair Conductor (ACSR/TP), ASTM International," American Society for Testing and Materials, West Conshohocken, PA, Standard, 2016.

[16] "Standard Specification for Pipe, Steel, Black and Hot-Dipped, Zinc-Coated, Welded and Seamless," American Society for Testing and Materials, West Conshohocken, PA, Standard, 2018.

[17] V. A. Rakov and A. Borghetti, *Brochure 549 - Lightning Parameters for Engineering Applications*. CIGRÉ, 2013, no. August.